Electrochimica Acta 54 (2009) 6680–6685

Contents lists available at ScienceDirect

Electrochimica Acta

journal homepage: www.elsevier.com/locate/electacta

Effects of microwave radiation on electrodeposition processes at tin-doped indium oxide (ITO) electrodes

Liza Rassaei [a], Elena Vigil [b], Robert W. French [a], Mary F. Mahon [a], Richard G. Compton [c], Frank Marken [a,*]

[a] Department of Chemistry, University of Bath, Bath BA2 7AY, UK
[b] Facultad de Fisica, Insituto de Ciencia y Tecnologia de Materiales, Universidad de La Habana, Ciudad Habana 10400, Cuba
[c] Physical and Theoretical Chemistry Laboratory, University of Oxford, South Parks Road, Oxford OX1 3QZ, UK

ARTICLE INFO

Article history:
Received 12 May 2009
Received in revised form 12 June 2009
Accepted 20 June 2009
Available online 28 June 2009

Keywords:
Microwave activation
Voltammetry
Electrodeposition
Titanium dioxide
Gold
Electroplating

ABSTRACT

In situ microwave activation is investigated for the electrodeposition of a metal (gold) and for a metal oxide (hydrous Ti(IV) oxide) onto tin-doped indium oxide (ITO) film electrodes. It is demonstrated that localized microwave heating of the ITO film can be exploited to affect electrodeposition processes.

The electrochemically reversible and temperature sensitive one-electron redox system $Fe(CN)_6^{3-/4-}$ was employed in aqueous solution in order to calibrate the average surface temperature at the ITO film electrode. In the presence of microwave radiation the average electrode surface temperature reached ca. 363 K whereas under the same conditions the bulk solution temperature reached ca. 313 K. Therefore localized heating of the ITO film appears to be important.

The rate of electrodeposition of gold from an aqueous 1 mM tetrachloroaurate(III) solution in 0.1 M KCl (adjusted to pH 2) is enhanced by microwave activation. However, the morphology of deposits remains un-effected. Hydrous titanium (IV) oxide films were electrodeposited from an aqueous solution of 1 mM $TiCl_3$ in 0.1 M acetate buffer pH 4.7. Dense films with blocking character were obtained with conventional heating but a fibrous more open deposit forms in the presence of microwaves.

1. Introduction

Microwave activation in chemistry has been employed successfully in a wide range of applications in materials chemistry [1], in organic [2] or inorganic [3] chemical synthesis, in analytical chemistry [4], and more recently in analytical electrochemistry [5]. Microwave radiation provides a unique tool to guide energy into localized reaction zones and to facilitate chemical processes [6]. In electrochemistry thermal effects are important [7] and localized heating has been investigated with conventional heating [8], for Rf-heated "hot wire" electrodes [9], Rf-heated microelectrodes [10] and channel flow systems [11], laser heating with front [12] or back [13] exposure, and for microwave heating [14].

Microwave activation experiments in electrochemical systems have usually been restricted to applications using focused microwave fields with heating effects localized only at the tip of microelectrodes [15]. The benefits of this experimental arrangement are fast on–off switching, negligible bulk heating, low power requirements, and safe operation. However, often electrochemical processes require larger electrodes and in particular electroplating processes require extended areas or more complex shapes. This study explores the effect of microwave radiation on electrochemical processes at tin-doped indium oxide (ITO) thin film electrodes. The absorption of microwave radiation by charge carriers in semiconductor or degenerate semiconductor materials is well known [16] and exploited here to create a localized heating effect. The deposition of a metal (gold) and the deposition of a metal oxide (hydrous Ti(IV) oxide) are employed as model cases.

2. Experimental details

2.1. Chemical reagents

Chemicals were obtained commercially in analytical grade and used without further purification. Tetrachloroauric(III) acid, potassium hydroxide, $K_4(Fe(CN)_6$, $K_3Fe(CN)_6$, and potassium chloride were purchased from Aldrich. A 15% solution of $TiCl_3$ in aqueous 10% hydrochloric acid was obtained from Merck. Deionized and filtered water of resistivity not less than 18 MΩ cm (at 20 °C) was taken from an Elga water purification system. Argon (BOC, UK) was employed for de-aeration of the electrolyte solutions.

2.2. Instrumentation

Electrochemical experiments were performed in a conventional three-electrode flow cell system using a micro-Autolab III

* Corresponding author. Tel.: +44 1225 383694; fax: +44 1225 386231.
E-mail address: F.Marken@bath.ac.uk (F. Marken).

0013-4686/$ – see front matter © 2009 Elsevier Ltd. All rights reserved.
doi:10.1016/j.electacta.2009.06.062

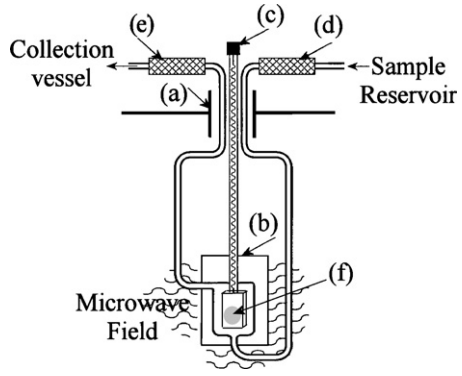

Fig. 1. Schematic drawing of the custom-made 10 cm^3 electrochemical glass cell (b) placed through a port (a) into the multi-mode microwave system. A flow system driven with a peristaltic pump (28 $cm^3\,min^{-1}$) was employed to pump electrolyte solution from a reservoir through the reference connection (d), through the cell, and out through the counter electrode (e) into the collection vessel. The working electrode (c) with an ITO slide attached (f) was placed from the top into the cell.

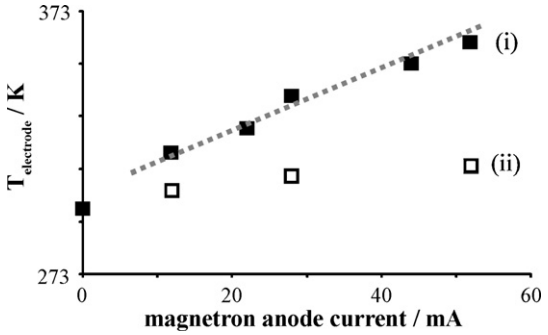

Fig. 2. Plot of (i) the average electrode temperature, $T_{electrode}$ (filled squares, estimated from the equilibrium potential in aqueous solution of 5 mM $Fe(CN)_6^{3-}$/5 mM $Fe(CN)_6^{4-}$ in 0.1 M KCl) and (ii) the cell outlet temperature (empty squares) vs. the applied microwave intensity (as magnetron anode current).

system (Eco Chemie, NL). A saturated calomel electrode (SCE, Radiometer) was used as the reference electrode (upstream) and a platinum gauze electrode as the counter electrode (downstream). The working electrode was prepared from ITO-coated glass (tin-doped indium oxide films sputter coated onto glass, active area 10 mm × 10 mm, resistivity 15 Ω per square, ITO film thickness ca. 80 nm) obtained from Image Optics Components Ltd. (Basildon, Essex, UK). The ITO electrodes were rinsed with acetone and water, heat treated in a tube furnace (Elite Thermal Systems Ltd.) for 1 h at 500 °C, and re-equilibrated to ambient conditions before use. Voltammograms were recorded in staircase mode (0.67 mV step potential). The morphology of deposited mesoporous Au or TiO_2 films were characterized by scanning electron microscopy (SEM) with a JEOL JSM6480LV system. Samples were gold sputter coated prior the experiments. Powder diffraction data were recorded on a Bruker D8 diffractometer fitted with Goebal mirrors and a 0.2 mm beam slit.

For microwave activation experiments, a multi-mode microwave oven (Panasonic NN-3456, 2.45 GHz) with modified smooth power supply, a water energy sink, and a port for the electrochemical cell was used [17]. The microwave intensity was controlled via the anode current of the magnetron. A fast flowing electrolyte solution circulated with a peristaltic pump (Watson–Marlow, 28 $cm^3\,min^{-1}$) ensured stable temperature conditions during experiments. The working electrode (Fig. 1) consisted of an ITO slide with 1 cm^2 exposed surface area connected to a 200 μm diameter insulated copper wire with a silver epoxy contact. *Special care is required when inserting metal objects into microwave systems and experiments should always be conducted at low power. Before and during operation, the system was monitored for leaking microwave radiation with an Apollo radiation meter.*

For comparison additional experiments were conducted in a thermostated water bath (Haake) employing the same electrochemical cell but with no flow to allow temperature equilibration.

2.3. Temperature calibration procedure

The average temperature at the ITO electrode surface, $T_{electrode}$, was determined based on the shift in equilibrium potential for an aqueous solution containing 5 mM $Fe(CN)_6^{3-}$ and 5 mM $Fe(CN)_6^{4-}$ in 0.1 M KCl. First the equilibrium potential was monitored as a function of temperature during conventional heating in a thermostated cell giving a temperature coefficient $dE/dT = -1.54\,mV\,K^{-1}$ as reported in the literature [18]. The shift in equilibrium potential was then measured as a function of applied microwave power (magnetron anode current) and a calibration graph determined (see Fig. 2(i)). During microwave experiments a considerable level of bulk heating was observed and in order to distinguish bulk heating from electrode surface heating also the outlet temperature of electrolyte solution leaving the electrochemical cell was monitored (see plot in Fig. 2(ii)).

2.4. Electrodeposition procedures

2.4.1. Gold electrodeposition

Gold(III) chloride hydrate was dissolved in 0.1 M KCl in deionized water and then the pH was adjusted to approximately 2 by addition of 1 M HCl. For continuous gold deposition, a potential of 0.4 V vs. SCE was applied for a duration of 900 s.

2.4.2. Hydrous Ti(IV) oxide electrodeposition

The electrodeposition solution was an aqueous 1 mM $TiCl_3$ prepared by dilution of a 15% solution of $TiCl_3$ in aqueous 10% hydrochloric acid. The pH of the solution was adjusted to 4.7 by addition of 0.1 M sodium acetate solution. The Ti(III) solution was kept under an atmosphere of argon in order to prevent the oxidation to Ti(IV) by oxygen. Fresh solutions were prepared to minimise the formation of colloid. Voltammetric scans were recorded (vide infra) and anodic deposition was observed over the entire potential range. Therefore the deposition of hydrous Ti(IV) oxide was carried out by continuously recorded cyclic voltammograms with a scan rate of 50 $mV\,s^{-1}$ over a −0.7 to +1.2 V vs. SCE potential range and for a specified number of potential cycles.

3. Results and discussion

3.1. Microwave-induced effects on the electrochemical reduction/oxidation of $Fe(CN)_6^{3-/4-}$ at a tin-doped indium oxide (ITO) electrode

The effect of applied microwave radiation on the mass transport and temperature conditions at solution-immersed metal electrodes with a diameter of less than 1 mm has been studied [5] and the size of the electrode has been shown to strongly affect local heating effects [19]. The volume of liquid directly affected by the focused microwave field at the tip of the metal electrode scales approximately with r^3 (where r is the electrode radius) and therefore energy requirements are hugely dependent on electrode diameter. With an electrode diameter bigger than 1 mm, the level of microwave power required to induce thermal effects is very high and the focusing effect induced by the metal electrode becomes insufficient when compared to the bulk liquid heating effect for aqueous electrolyte media. However, for thin film electrodes with high surface area

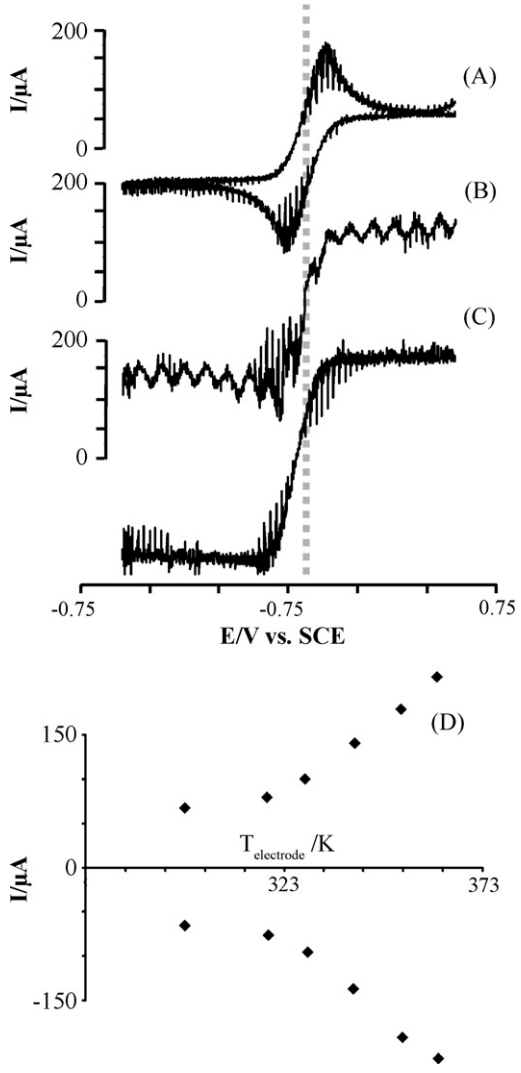

Fig. 3. Cyclic voltammograms (scan rate 10 mV s^{-1}) for the oxidation/reduction of 1 mM $Fe(CN)_6^{4-}$/1 mM $Fe(CN)_6^{3-}$ at a 1 cm^2 ITO electrode in aqueous 0.1 M KCl (A) in the absence, and (B) in the presence of 4 s pulsed and (C) continuous microwave radiation (magnetron anode current 52 mA corresponding to an average temperature of 83 °C). (D) Plot of the mass transport controlled limiting currents for the oxidation of $Fe(CN)_6^{4-}$ and for the reduction of $Fe(CN)_6^{3-}$ vs. temperature (in the presence of microwaves, see calibration plot in this figure).

localized microwave-induced temperature effects may be possible due to the direct interaction of the conducting or semiconducting film with microwave radiation. Here, a thin tin-doped indium oxide (or ITO) layer (ca. 80 nm conducting ITO film thickness by SEM) on a glass slide is employed with an exposed electrode area of ca. 1 cm^2. Initially, the effect of microwave radiation on temperature and mass transport are assessed by employing the one-electron $Fe(CN)_6^{3-/4-}$ redox system (see Eq. (1)).

$$Fe(CN)_6^{3-}(aq) + e^- \rightleftarrows Fe(CN)_6^{4-}(aq) \quad (1)$$

The oxidation and reduction of $Fe(CN)_6^{3-/4-}$ in aqueous 0.1 M KCl is shown in Fig. 3. In the absence of microwave radiation (see Fig. 3A) well-defined current peaks are observed even at a scan rate of 10 mV s^{-1} with a midpoint potential $E_{mid} = E_p^{ox} + E_p^{red}/2$ of ca. 0.075 V vs. SCE (see dotted line in Fig. 3). The limiting currents for oxidation (at more positive potentials) and for reduction (at more negative potential) are 90 and −75 μA, respectively, indicating that convection in the flow cell occurs close to the electrode surface. The "noise" pattern superimposed on the voltammetric signal is caused by the peristaltic pump system which is required to maintain uniform temperature conditions during experiments.

Upon application of microwave radiation to the electrochemical system, a gradual increase of currents with microwave intensity is observed (see Fig. 3D). Fig. 3C shows a typical cyclic voltammogram obtained with continuous microwave heating. The peak features have disappeared and a well-defined steady state current response is observed with a characteristic shift in the reversible potential towards more negative values (due to the increase in temperature, vide supra). The response time of the electrode system to microwave pulses provides a measure of the zone of liquid that is heated. For small electrodes very short temperature rise times are obtained [17] but for larger electrodes a much slower response is expected. Fig. 3B shows a voltammogram recorded in the presence of 4 s microwave pulses. The decay of current during the "off" period does not reach the room temperature current limit and the rise in current during the "on" period does not reach the limiting current observed under continuous microwave radiation (see Fig. 3C). Therefore the response time of the electrode system is in the order of 10 s and in order to reach thermal equilibrium (with electrolyte flowing through the cell) 10–20 s are required.

The delayed response of the electrode system to microwave pulses is an indication for a heating effect due to both (i) direct microwave heating of the ITO electrode film in contact with the solution phase and (ii) heating of the bulk electrolyte solution during transit through the cell. The relative contribution from these two heating mechanisms can be assessed by determining the bulk liquid temperature at the outlet of the electrochemical cell. This "outlet temperature calibration" measurement is contrasted to the "electrode surface temperature calibration" in the plot in Fig. 2. The bulk temperature reaches approximately 313 K when the electrode surface temperature is approximately 363 K. This difference suggests that substantial localized heating occurs due to absorption of microwave energy in the ITO film electrode.

3.2. Microwave-induced effects on the electrochemical deposition of gold at a tin-doped indium oxide (ITO) electrode

Electrodeposition processes can be applied for a wide range of materials including metals [20], metal oxides [21], polymers [22], or semiconductors [23]. Often wet electrodeposition offers practical advantages over high vacuum or gas phase deposition in industrial processes. Control over electrodeposition processes is desirable to improve film quality and deposition rate. Here, microwave activation is applied first to a metal deposition process and then to a metal oxide deposition in order to assess effects.

The electrodeposition of gold is a well known process employed for the formation of catalytic nanoparticles [24], for paired electrode junctions [25], and to form nanostructures [26]. There are several types of gold plating baths [27] but here a simple dilute hydrochloric acid medium is chosen to investigate gold electrodeposition in the presence of microwave radiation.

Gold deposits are grown on the surface of an ITO substrate electrode in the absence and in the presence of microwave radiation. Fig. 4A shows data from cyclic voltammetry experiments for electrodeposition of gold from aqueous 1 mM tetrachloroaurate(III) solution in 0.1 M KCl (adjusted to pH 2). The deposition of gold commences at ca. 0.4 V vs. SCE. A reduction peak is observed and the current levels off. After reversal of the scan direction a typical nucleation loop is observed and the gold stripping process commences at ca. 0.8 V vs. SCE. Increasing the temperature to 343 K (see Fig. 4A(ii)) causes an increase in peak and deposition current and an earlier onset of the stripping process. The nucleation of the gold deposit appears to be only weakly affected.

Under microwave conditions flow of solution through the electrochemical cell is imposed with a peristaltic pump system in order

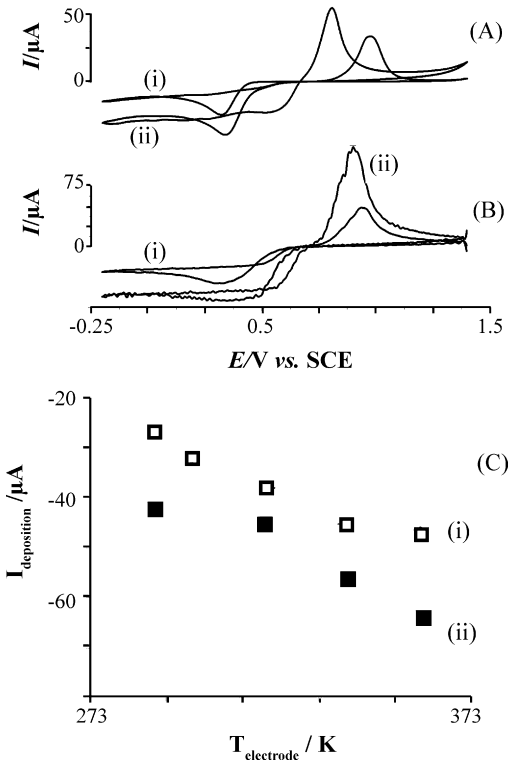

Fig. 4. Cyclic voltammograms (scan rate 0.02 V s^{-1}) obtained for the reduction and re-oxidation of 1 mM $AuCl_4^-$ in aqueous 0.1 M KCl at pH 2 (pH adjusted with HCl) at an ITO-coated glass electrode (1 cm^2) (A) in a thermal bath without flow (i) at 298 K and (ii) at 343 K and (B) in the presence of microwave radiation (with 28 cm^3 min^{-1} flow, magnetron current (i) 0 mA and (ii) 28 mA). (C) Plot of the peak current for the reduction of $AuCl_4^-$ (i) in a thermal bath without flow and (ii) in the presence of microwave with 28 cm^3 min^{-1} flow.

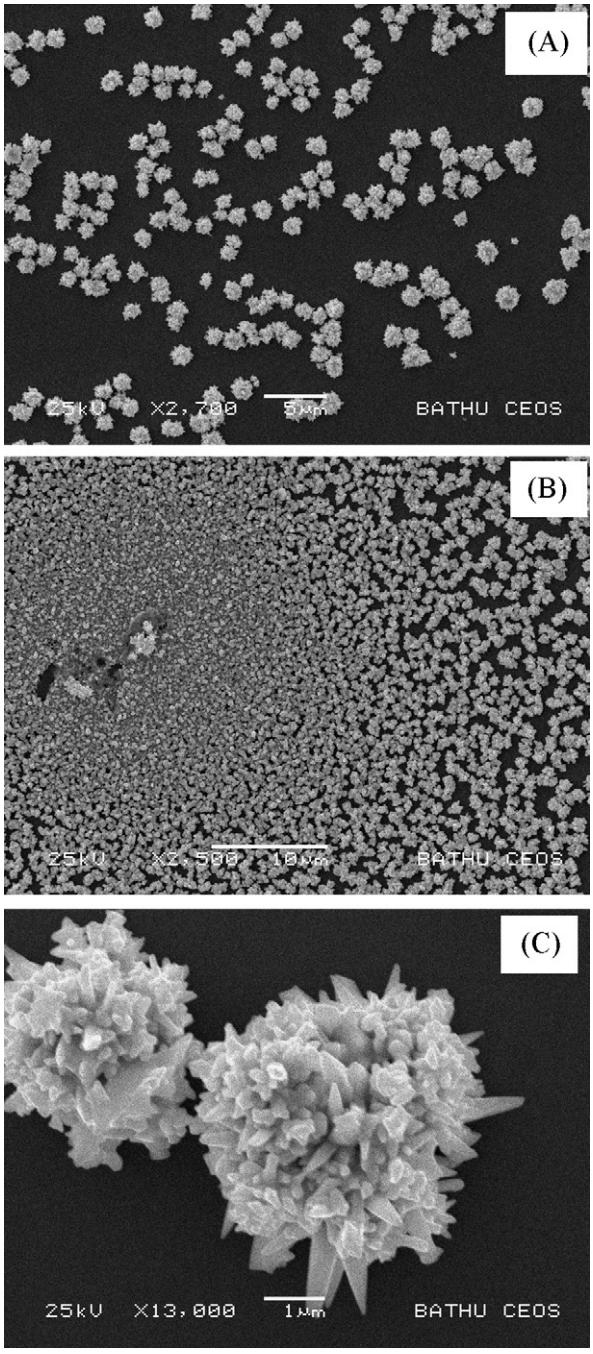

Fig. 5. SEM images of gold deposits grown from a solution of 1 mM $AuCl_4^-$ in 0.1 M KCl (adjusted to pH 2 with HCl) onto ITO electrode substrates (A) at room temperature in stagnant solution and (B and C) in the presence of microwave radiation (flow 28 cm^3 min^{-1}, 52 mA anode current corresponding to 363 K).

to maintain a stable temperature. As a result currents for the gold deposition process are enhanced already at room temperature (see Fig. 4B(i)). In the presence of microwave radiation a further increase in current is observed (see Fig. 4B(ii)). The effects are summarized in Fig. 4C which shows the approximately linear increase in gold deposition current with temperature.

Fig. 5 shows typical SEM images of gold deposits grown onto ITO electrodes at different temperatures and in absence or presence of microwave radiation. It can be seen that the morphology of gold deposits is very similar under all conditions. The effect of the temperature is to increase the density of the gold deposit (due to an increased rate of nucleation) but the effect is not very strong and comparable to the effect introduced by flow.

In summary, the electrodeposition of gold onto ITO can be enhanced by microwave radiation and the density of the deposit can be increased. However, the effects on the morphology of the gold deposit are small.

3.3. Microwave-induced effects on the electrochemical deposition of hydrous titanium oxide at a tin-doped indium oxide (ITO) electrode

Titanium dioxide, TiO_2, is widely known as an important electrode material in semiconductors [28], for photocatalysis [29], solar cells [30], and biosensors [31]. Most of these useful functions depend mainly on the composition, configuration, and structure of TiO_2. Many methods have been used to prepare TiO_2 thin films such as magnetron sputtering deposition [32], sol–gel [33], electrodeposition [34], and chemical vapour deposition [35]. Among these methods, electrodeposition of TiO_2 is attractive because electrochemical deposition allows thickness and morphology control by varying the electroplating parameters [36]. The effect of microwave radiation on the chemical (electroless) solution deposition of TiO_2 has been reported by Vigil and co-workers [37–39].

A literature strategy for the electrochemical formation of TiO_2 at electrode surfaces is to employ a $TiCl_3$ precursor which is soluble in aqueous media and which upon oxidation at the electrode surface rapidly hydrolyses into a hydrous oxide deposit [40]. Kavan et al. [41] and Manivannan et al. [42] suggested the use of a hydrochloric acid medium for the electrodeposition of hydrous TiO_2. However, at elevated temperature a solution of $TiCl_3$ in aqueous HCl pH 2 is etching the ITO electrode film and therefore more mild condi-

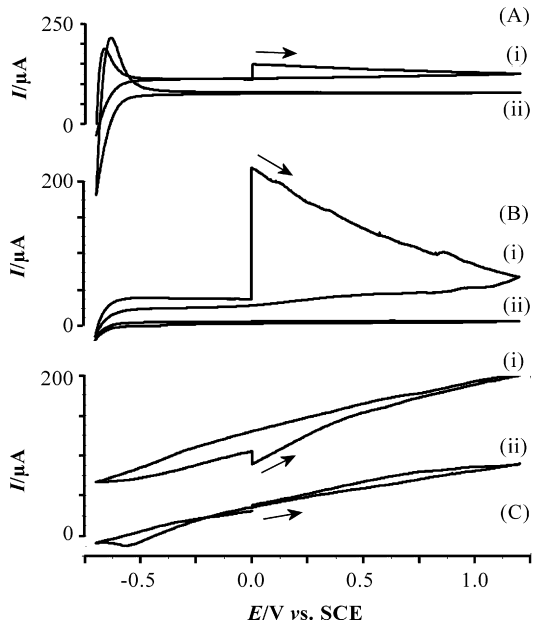

Fig. 6. Multi-cycle voltammograms (scan rate 0.05 V s^{-1}, (i) first potential cycle, (ii) 10th potential cycle) obtained for the oxidation of $TiCl_3$ in aqueous 0.1 M acetate buffer at pH 4.7 at an ITO film electrode (area 1 cm^2) (A) in a thermostated bath at room temperature, (B) in a thermostatted bath at 353 K, and (C) in the presence of microwave radiation (flow 28 $cm^3 min^{-1}$, magnetron anode current 52 mA corresponding to $T_{electrode}$ = 353 K).

tions had to be investigated. A solution of $TiCl_3$ in acetate buffer pH 4.7 was chosen. Cyclic voltammograms in Fig. 6A show typical responses observed during the deposition process. Initially, a positive current is observed (see Fig. 6A(i)) over the entire potential range. The positive current is associated with the oxidation of Ti(III) to Ti(IV) and the current gradually diminishes due to film deposition at the electrode surface. At more negative potentials at ca. −0.5 V vs. SCE a typical reversible TiO_2 film response is observed [43] and this voltammetric response is increasing with deposition time thereby indicating growth of a titanium oxide film (see Fig. 6A(ii)). At elevated temperatures (353 K, see Fig. 6B(i)) the deposition process is faster and the decay of the anodic deposition current is more rapid. After 10 consecutive potential cycles the current is almost zero due to the formation of the insulating TiO_2 film. The film material without calcination is X-ray amorphous and therefore likely to contain highly hydrated TiO_2. The voltammetric response for the TiO_2 deposit at negative potential is irreversible (consistent with enhanced hydrogen evolution) at elevated temperatures (see Fig. 6B).

In the presence of microwaves and under flow conditions a similar anodic deposition process can be observed (see Fig. 6C). The deposition current gradually diminishes although even after 10 consecutive potential cycles there is still a clear deposition current observed.

SEM images of the deposits are shown in Fig. 7. Under conventional deposition conditions a film deposit with granular appearance is observed and crazing occurs in particular for thicker deposits (see Fig. 7B). Films deposited under microwave conditions exhibit a different morphology with fibrous components and a much more open and porous structure. This more open structure explains the continuing deposition with less blocking

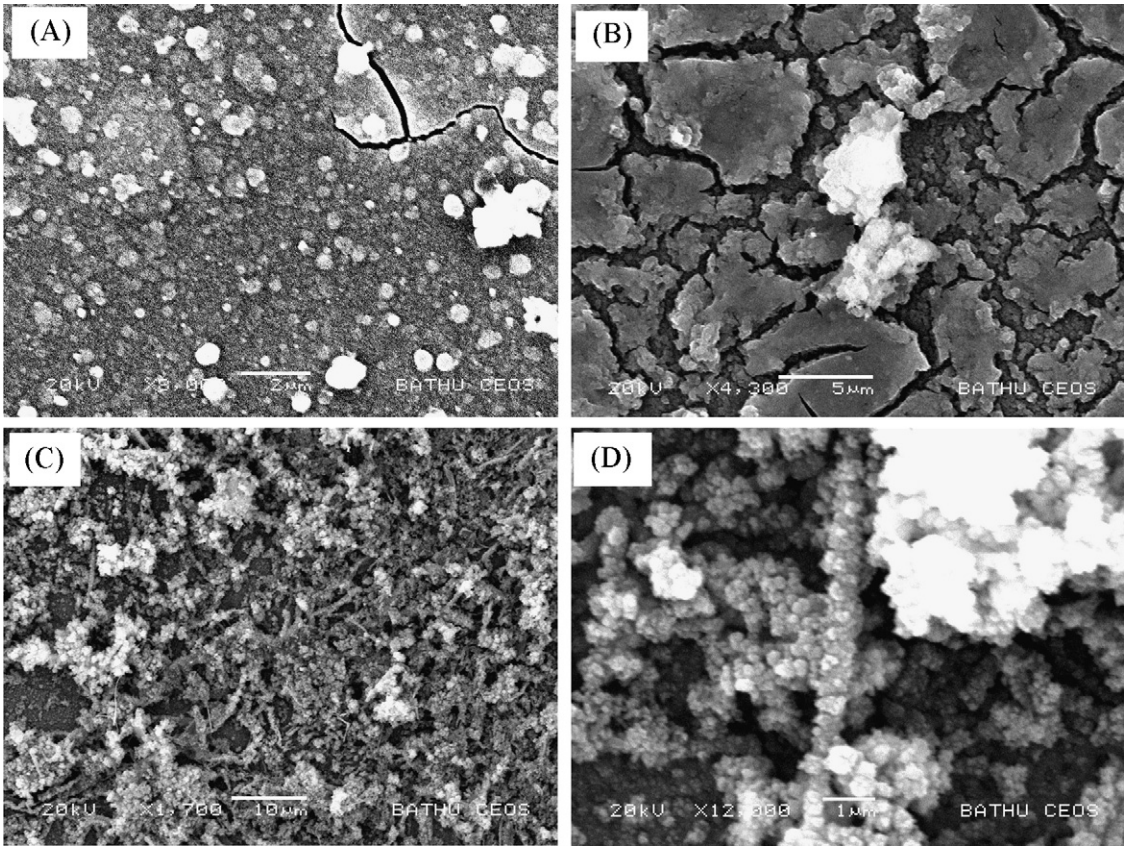

Fig. 7. SEM images showing (A) a TiO_2 film deposited in stagnant solution at 293 K, (B) a TiO_2 film deposited in stagnant solution at 363 K, and (C and D) a TiO_2 film deposited in flowing solution in the presence of microwaves (300 mA magnetron anode current corresponding to 353 K).

under microwave conditions. The formation of the fibrous components may be in part caused by the enhanced deposition of colloidal titanium oxide material which could be enhanced by local dieletrophoretic effects.

The hydrous titanium oxide films grown by electrodeposition are X-ray amorphous and only after calcination at 500 °C can the TiO_2 (anatase) structure be clearly observed in the XRD pattern. Unfortunately, the fibrous morphology of the deposit is destroyed by heating already at 300 °C and the resulting films after calcination are porous but more uniform (not shown). The crazing effect (see Fig. 6B) which is associated with density changes during calcination can be avoided when using microwave activation during deposition.

4. Conclusion

It has been shown that microwave enhanced electrodeposition processes are observed when ITO-coated glass slides are employed as electrodes. A flowing electrolyte system is necessary to stabilise temperature gradients within the electrochemical cell and average electrode temperatures of ca. 363 K were obtained. For both gold and hydrous titanium oxide deposition, enhanced deposition rates were observed. For the deposition of hydrous titanium oxide also a morphology change to a more fibrous deposit was observed. In future a wider range of thin film electrodes could be studied under microwave conditions and the effects of electrode film thickness and electrolyte concentration employed to improve the electrodeposition process. The deposition of a wider range of oxide materials and in particular semiconducting materials could be studied to establish applications for microwave effects during electrodeposition.

Acknowledgement

The authors would like to thank the EPSRC for financial support (EP/F025726/1).

References

[1] G.A. Tompsett, W.C. Conner, K.S. Yngvesson, Chem. Phys. Chem. 7 (2006) 296.
[2] A. Loupy (Ed.), Microwaves in Organic Synthesis, Wiley-VCH, Weinheim, 2006.
[3] D.M.P. Mingos, D.R. Baghurst, Chem. Soc. Rev. 20 (1991) 1.
[4] H.M. Skip Kingston, S.J. Haswell (Eds.), Microwave-Enhanced Chemistry: Fundamentals, Sample Preparation, and Applications, American Chemical Society, Washington, 1997.
[5] I.J. Cutress, F. Marken, R.G. Compton, Electroanalysis 21 (2009) 113.
[6] C. Gabriel, S. Gabriel, E.H. Grant, B.S.J. Halstead, D.M.P. Mingos, Chem. Soc. Rev. 27 (1998) 213.
[7] F. Marken, U.K. Sur, B.A. Coles, R.G. Compton, Electrochim. Acta 51 (2006) 2195.
[8] G.G. Wildgoose, N.S. Lawrence, B.A. Coles, L. Jiang, T.G.J. Jones, R.G. Compton, Phys. Chem. Chem. Phys. 5 (2003) 4219.
[9] P. Gründler, G.U. Flechsig, Microchim. Acta 154 (2006) 175.
[10] A. Boika, A.S. Baranski, Anal. Chem. 80 (2008) 7392.
[11] B.A. Coles, M.J. Moorcroft, R.G. Compton, J. Electroanal. Chem. 513 (2001) 87.
[12] V. Climent, N. Garcia-Araez, R.G. Compton, J.M. Feliu, J. Phys. Chem. B 110 (2006) 21092.
[13] J.F. Smalley, L. Geng, A. Chen, S.W. Feldberg, N.S. Lewis, G. Cali, J. Electroanal. Chem. 549 (2003) 13.
[14] F. Marken, Ann. Rep. Prog. Chem. Sect. C: Phys. Chem. 104 (2008) 124.
[15] L. Rassaei, R.G. Compton, F. Marken, J. Phys. Chem. C 113 (2009) 3046.
[16] M.J. Cass, N.W. Duffy, L.M. Peter, S.R. Pennock, S. Ushiroda, A.B. Walker, J. Phys. Chem. B 107 (2003) 5857.
[17] U.K. Sur, F. Marken, N. Rees, B.A. Coles, R.G. Compton, R. Seager, J. Electroanal. Chem. 573 (2004) 175.
[18] M.A. Ghanem, M. Thompson, R.G. Compton, B.A. Coles, S. Harvey, K.H. Parker, D. O'Hare, F. Marken, J. Phys. Chem. B 110 (2006) 17589.
[19] M.A. Ghanem, R.G. Compton, B.A. Coles, A. Canals, A. Vuorema, P. John, F. Marken, Phys. Chem. Chem. Phys. 7 (2005) 3552.
[20] M.A. Ghanem, H. Hanson, R.G. Compton, B.A. Coles, F. Marken, Talanta 72 (2007) 66.
[21] F. Marken, Y.C. Tsai, A.J. Saterlay, B.A. Coles, D. Tibbetts, K. Holt, C.H. Goeting, J.S. Foord, R.G. Compton, J. Solid State Electrochem. 5 (2001) 313.
[22] I. Zhitomirsky, J. Mater. Sci. 41 (2006) 8186.
[23] G.Z. Cao, D.W. Liu, Adv. Coll. Interface Sci. 136 (2008) 45.
[24] R. Baron, G.G. Wildgoose, R.G. Compton, J. Nanosci. Nanotechnol. 9 (2009) 2274.
[25] R.W. French, A.M. Collins, F. Marken, Electroanalysis 20 (2008) 2403.
[26] J. Burdick, E. Alonas, H.C. Huang, K. Rege, J. Wang, Nanotechnology 20 (2009) 065306.
[27] M. Schlesinger, M. Paunovic (Eds.), Modern Electroplating, Wiley, New York, 2000, p. 205.
[28] Y. Nakato, A. Tsumura, H. Tsubomura, J. Phys. Chem. 87 (1983) 2402.
[29] A. Fujishima, T.N. Rao, D.A. Tryk, J. Photochem. Photobiol. C 1 (2000) 1.
[30] L.M. Peter, Phys. Chem. Chem. Phys. 9 (2007) 2630.
[31] S. Cosnier, A. Senillou, M. Grätzel, P. Comte, N. Vlachopoulos, N.J. Renault, C. Martelet, J. Electroanal. Chem. 469 (1999) 176.
[32] S. Kment, P. Kluson, V. Stranak, P. Virostko, J. Krysa, M. Cada, J. Pracharova, M. Kohout, M. Morozova, P. Adamek, Z. Hubicka, Electrochim. Acta 54 (2009) 3352.
[33] Y.H. Liao, J.C. Chou, Mater. Chem. Phys. 114 (2009) 542.
[34] S. Karuppuchamy, N. Suzuki, S. Ito, T. Endo, Curr. Appl. Phys. 9 (2009) 243.
[35] E. Halary-Wagner, T. Bret, P. Hoffmann, Appl. Surf. Sci. 208–209 (2003) 663.
[36] C.C. Hu, C.C. Huang, K.H. Chang, Electrochem. Commun. 11 (2009) 434.
[37] E. Vigil, J.A. Ayllon, A.M. Peiro, R. Rodriguez-Clemente, X. Domenech, J. Peral, Langmuir 17 (2001) 891.
[38] E. Vigil, B. Gonzalez, I. Zumeta, S. Docteur, A.M. Peiro, D. Gutierrez-Tauste, C. Domingo, X. Domenech, J.A. Ayllon, J. Cryst. Growth 262 (2004) 366.
[39] I. Zumeta, B. Gonzalez, R. Espinosa, J.A. Ayllon, E. Vigil, Semicond. Sci. Technol. 19 (2004) L52.
[40] S. Cassaignon, M. Koelsch, J.P. Jolivet, J. Phys. Chem. Solids 68 (2007) 695.
[41] L. Kavan, B. Oregan, A. Kay, M. Grätzel, J. Electroanal. Chem. 346 (1993) 291.
[42] A. Manivannan, N. Spataru, K. Arihara, A. Fujishima, Electrochem. Solid State Lett. 8 (2005) C138.
[43] E.V. Milsom, A.M. Bond, A.P. O'Mullane, D. Elton, C.Y. Lee, F. Marken, Electroanalysis 21 (2009) 41.